sensors

MDPI

Article

Control Circuits for Potentiostatic/Galvanostatic Polarization and Simultaneous Chemical Sensing by a Light-Addressable Potentiometric Sensor

Tatsuo Yoshinobu [1,*], Rintaro Ikeda [2] and Ko-ichiro Miyamoto [2]

[1] Department of Biomedical Engineering, Tohoku University, Sendai 980-8579, Japan
[2] Department of Electronic Engineering, Tohoku University, Sendai 980-8579, Japan; koichiro.miyamoto.d2@tohoku.ac.jp (K.-i.M.)
* Correspondence: tatsuo.yoshinobu.a1@tohoku.ac.jp

Abstract: A light-addressable potentiometric sensor (LAPS) is a semiconductor-based sensor platform for sensing and imaging of various chemical species. Being a potentiometric sensor, no faradaic current flows through its sensing surface, and no electrochemical reaction takes place in the course of LAPS measurement. In this study, a four-electrode system is proposed, in which a LAPS is combined with the conventional three-electrode electrochemical system. A LAPS is included as the fourth electrode for potentiometric sensing and imaging of the target analyte in the course of an electrochemical reaction taking place on the surface of the working electrode. The integrated system will be useful for analyzing dynamic processes, where both the electrochemical process on the electrode surface and the ion distribution in the solution need to be simultaneously investigated. Different grounding modes of control circuits that can simultaneously conduct potentiostatic/galvanostatic polarization and LAPS measurement are designed, and their functionalities are tested. The interference between polarization and LAPS measurement will also be discussed.

Keywords: light-addressable potentiometric sensor; LAPS; pH sensor; chemical sensor; faradaic current; potentiostat; galvanostat; polarization; electrochemical system; corrosion

Citation: Yoshinobu, T.; Ikeda, R.; Miyamoto, K.-i. Control Circuits for Potentiostatic/Galvanostatic Polarization and Simultaneous Chemical Sensing by a Light-Addressable Potentiometric Sensor. *Sensors* **2024**, *24*, 5666. https://doi.org/10.3390/s24175666

Academic Editor: Peng Miao

Received: 16 July 2024
Revised: 27 August 2024
Accepted: 29 August 2024
Published: 30 August 2024

1. Introduction

A light-addressable potentiometric sensor (LAPS) [1–7] is a semiconductor-based chemical sensor in which the variation of the potential on the sensing surface in response to the analyte is detected in the form of an alternating current (AC) signal. Figure 1a shows a typical measurement setup of a LAPS, in which the sensor plate is virtually grounded via an ammeter that measures the AC signal i_{sig}. The bias voltage V_{bias} applied between the reference electrode (RE) and the LAPS induces a depletion layer in the semiconductor, the width of which varies in response to the surface potential. Under this situation, the semiconductor layer is illuminated with a periodically modulated light beam, which generates the photocurrent signal i_{sig} to be correlated with the activity of the target analyte. The light-addressability is the most remarkable feature and the advantage of a LAPS, which makes it possible to conduct the measurement in a spatially resolved manner. Based on this feature, various chemical imaging sensor systems have been realized with a LAPS sensor plate scanned by a focused light beam [8–14].

A LAPS is a potentiometric sensor, in which no direct current flows through the insulated sensing surface, and no electrochemical reaction occurs as a result of the measurement. A LAPS measurement can, therefore, be said to be non-destructive in the sense that the measurement does not change the sample solution to be measured. On the other hand, it can also be a limitation because an electrode for a faradaic current to flow through is needed for analysis of a system in which an electrochemical reaction is taking place. There can be two approaches to realizing an electrochemical system with light-addressability. One

approach is to combine a LAPS measurement system with a conventional three-electrode system, as shown in Figure 1b, resulting in a four-electrode system, as shown in Figure 1c. We previously employed such a configuration for pH imaging in the vicinity of a corroding metal surface under potentiostatic polarization [15–17]. The faradaic current flowing out from the working electrode (WE) will be collected by the counter electrode (CE), which also collects the AC signal from the LAPS. The other approach is to make the WE itself light-addressable. The light-addressable electrode (LAE) [18–21], the light-addressable amperometric sensor (LAAS) [22–27], the light-activated electrochemistry (also LAE) [28–31], and the photoelectrochemical imaging system (PEIS) [32–34] are examples of the latter approach, in which a faradaic current flows at the illuminated location on the electrode surface, which is not insulated.

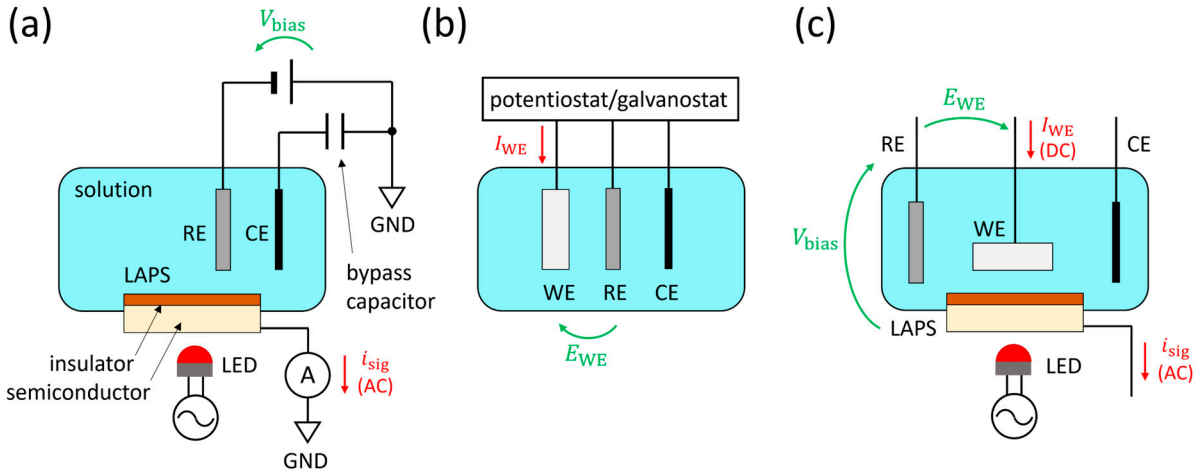

Figure 1. Schematics of electrode configurations of (**a**) a typical LAPS measurement system, (**b**) a conventional three-electrode system, and (**c**) a combined four-electrode system. An example of the real-space configuration of the four-electrode system is shown later in Section 4. LAPS, light-addressable potentiometric sensor; LED, light-emitting diode; RE, reference electrode; WE, working electrode; CE, counter electrode; GND, ground; AC, alternating current; DC, direct current.

This paper focuses on the circuit design of the four-electrode system mentioned above, which allows both potentiostatic and galvanostatic polarization of the WE and a simultaneous LAPS measurement in different grounding modes. Integration of LAPS in an electrochemical system allows a spatiotemporal interrogation of the ion distribution in the solution, in which an electrochemical reaction is taking place on the WE surface. The integrated system will be useful for analyzing dynamic processes, where both the electrochemical process on the electrode surface and the ion distribution in the solution need to be simultaneously investigated.

2. Circuit Design

2.1. Requirements

The basic requirements for the four-electrode system are as follows. For LAPS measurement, a bias voltage V_{bias} is applied between the RE and the LAPS so that the potential of the semiconductor substrate of the LAPS will be $-V_{bias}$ vs. RE. The bias voltage V_{bias} is either constant or scanned in a typical range of −2 V to +2 V. As the surface of a LAPS is insulated, no direct current flows and only an AC photocurrent i_{sig} flows, which is typically of the order of μA. The frequency of i_{sig} is the same as the modulation frequency of the light beam, which is typically in the range of 100 Hz to 100 kHz. In potentiostatic polarization, the potential of the WE is controlled at a specified value E_{WE} vs. RE, and the resulting current flowing out of the WE, I_{WE}, is monitored. In galvanostatic polarization, the current flowing out of the WE is controlled at a specified value I_{WE}, and the resulting E_{WE} is monitored. In both cases, the target values are either constant or only slowly changing. The

value of E_{WE} is typically in the range of −10 V to +10 V, whereas the magnitude of I_{WE} may very much differ depending on the system under polarization.

2.2. Grounding Modes

Two grounding modes of circuits are designed to meet different requirements of the electrochemical system and the LAPS measurement. In the first type of control circuit, the LAPS is virtually grounded via a transimpedance amplifier (TIA), which measures i_{sig}. In most cases, this grounding mode is preferable because it is advantageous to stabilize the potential of the LAPS for the precise measurement of i_{sig}, which is small. In the second type of control circuit, the WE is virtually grounded. This control circuit can be used when it is necessary, for some reason, to keep the WE at the ground potential (GND). The functions of the LAPS-grounded and the WE-grounded control circuits are identical except for their grounding modes.

2.3. Control Schemes

Considering the combinations of the two grounding modes (LAPS-grounded and WE-grounded) and the two control modes (potentiostatic and galvanostatic), four control schemes were designed, as summarized in Figure 2. In these simplified diagrams, the values in blue and red show the input and output parameters, respectively. In all cases, V_{bias} is given as an input, and i_{sig} is read out as an output. E_{WE} and I_{WE} are input and output parameters, respectively, in a potentiostatic mode (PS mode) and vice versa in a galvanostatic mode (GS mode). The values in green show the potentials of the electrodes vs. GND.

The operation of each control circuit is briefly described below. Figure 2a,b shows simplified diagrams of the LAPS-grounded potentiostat and galvanostat, respectively. In these circuits, the LAPS is virtually grounded via an ammeter, and the potential of the RE is controlled at V_{bias} vs. GND by an operational amplifier. In Figure 2a, the potential of the WE is set at V_{bias} + E_{WE} vs. GND, or equivalently, E_{WE} vs. RE, and I_{WE} is measured. In Figure 2b, the WE is connected to a current source $I_{WE,}$ and its potential E_{WE} vs. RE is monitored.

Figure 2c,d shows simplified diagrams of WE-grounded potentiostat and galvanostat, respectively. In Figure 2c, the WE is virtually grounded via an ammeter, which measures I_{WE}, and the potential of the RE is controlled at $-E_{WE}$ vs. GND by an operational amplifier so that the potential of the WE will be E_{WE} vs. RE. The potential of the LAPS is set at $-E_{WE}$ − V_{bias} vs. GND so that the potential of the RE will be V_{bias} vs. LAPS. In Figure 2d, the WE is virtually grounded by an operational amplifier. The WE is also connected to a current source I_{WE}, and E_{WE} is measured. The potential of the LAPS is set at $-E_{WE}$ − V_{bias} so that the potential of the RE will be V_{bias} vs. LAPS.

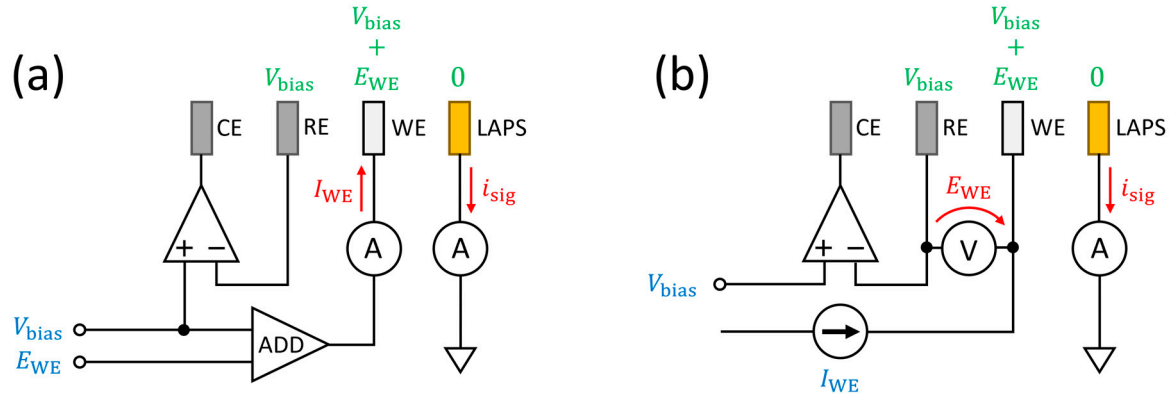

Figure 2. *Cont.*

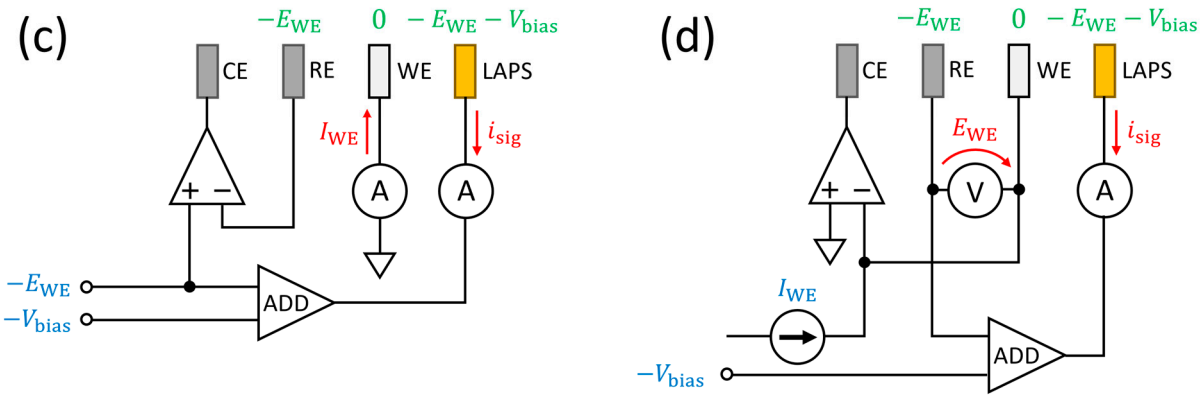

Figure 2. Simplified diagrams showing the control schemes of the four-electrode systems with different grounding modes for potentiostatic/galvanostatic polarization and simultaneous LAPS measurement. (**a**) A potentiostat with a virtually grounded LAPS. (**b**) A galvanostat with a virtually grounded LAPS. (**c**) A potentiostat with a virtually grounded WE. (**d**) A galvanostat with a virtually grounded WE. The values in blue and red show the input and output parameters, respectively, and the values in green show the potentials of the electrodes vs. GND. A unit labeled "ADD" is a voltage adder circuit.

3. Implementation

3.1. Potentiostat/Galvanostat with a Virtually Grounded LAPS

Figure 3a shows an example of a dual-functional circuit with a virtually grounded LAPS, which can be switched between the PS mode and the GS mode. The LAPS is virtually grounded by the TIA-1, which measures i_{sig} with a transimpedance gain determined by R_1. The TIA-1 can also be replaced with an external current preamplifier. In both the PS mode and the GS mode, the potential of the RE is controlled at V_{bias} by the operational amplifier OA-1. In the PS mode, the potential of the WE is set at V_{bias} + E_{WE} by the TIA-2, which measures I_{WE} with a transimpedance gain determined by R_2. In the GS mode, the loop composed of the ADD-2 and R_3 maintains the voltage difference across R_3 at the specified value $R_3 I_{WE}$ so that a current I_{WE} flows out of the WE.

The circuit was implemented on a printed circuit board (PCB) and operated with a power supply of ±12 V. The operational amplifiers used in TIAs were OP42GPZ (Analog Devices, Wilmington, MA, USA), and other operational amplifiers were OP07CPZ (Analog Devices, Wilmington, MA, USA). The instrumentation amplifiers LT1167CN8 (Linear Technology/Analog Devices, Wilmington, MA, USA) were used with a unity gain.

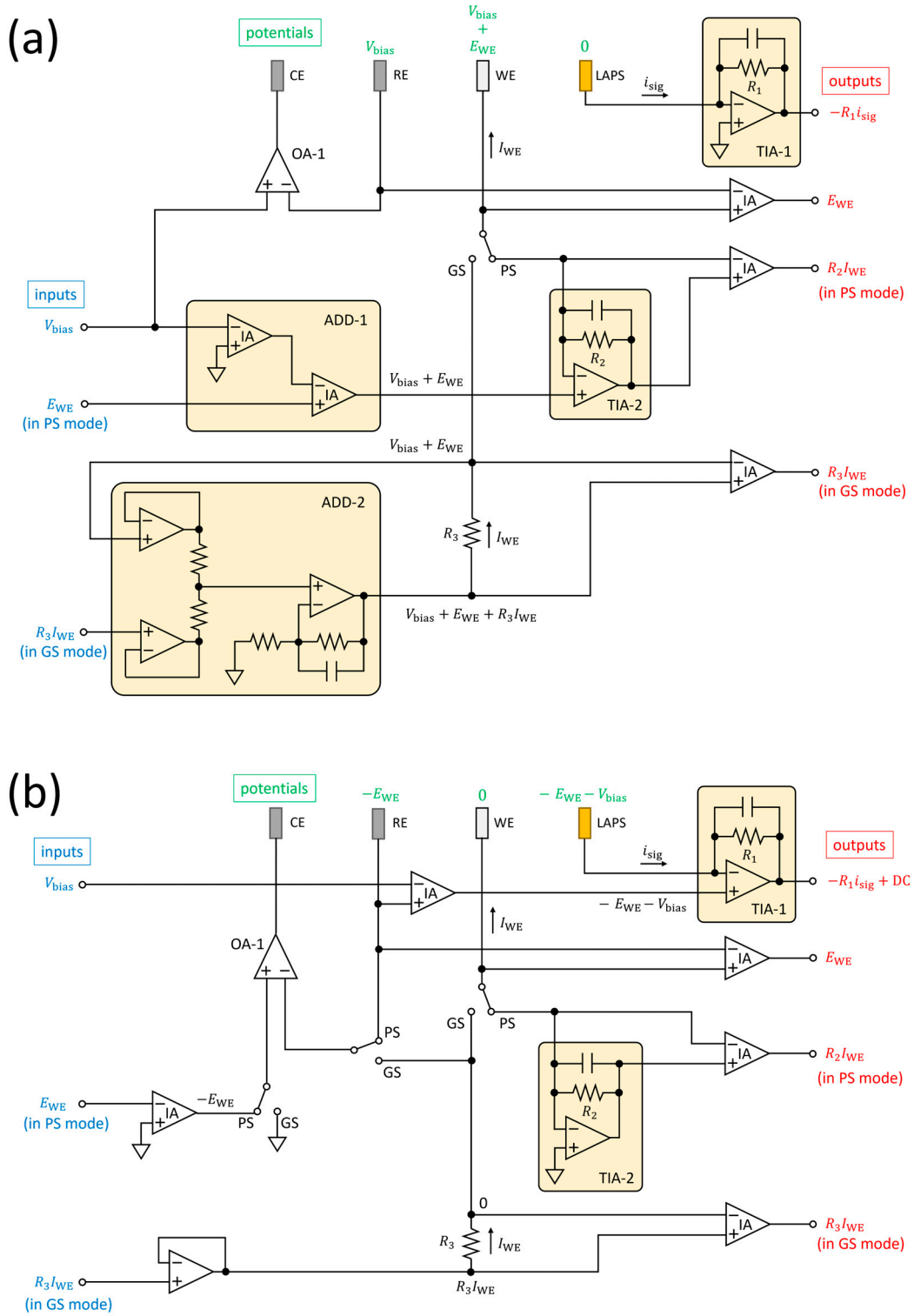

Figure 3. Diagrams of (**a**) LAPS-grounded and (**b**) WE-grounded control circuits for a four-electrode system, each of which can be switched between the PS mode and the GS mode. The power supply and the power supply bypass capacitors are omitted in the diagrams. The values in blue and red show the input and output parameters, respectively, and the values in green show the potentials of the electrodes vs. GND. All the instrumentation amplifiers are used with a unity gain, but those for monitor outputs can also be used with selective gains by connecting external resistances. OA, operational amplifier; IA, instrumentation amplifier; TIA, transimpedance amplifier; ADD, voltage adder circuit; PS, potentiostat; GS, galvanostat; GND, ground.

3.2. Potentiostat/Galvanostat with a Virtually Grounded WE

Figure 3b shows an example of a dual-functional circuit with a virtually grounded WE. In the PS mode, the WE is virtually grounded by the TIA-2, which measures I_{WE}. The OA-1 controls the potential of the RE at $-E_{WE}$ vs. GND so that the potential of the WE will be E_{WE} vs. RE. In the GS mode, the WE is virtually grounded by the OA-1. The current flowing out of the WE, I_{WE} is determined by the potential difference across R_3. In both the PS mode and the GS mode, the TIA-1 controls the potential of the LAPS at $-E_{WE} - V_{bias}$ so that the potential of the RE will be V_{bias} vs. LAPS. The TIA-1 measures i_{sig} with a transimpedance gain determined by R_1. It should be noted that the output of the TIA-1 has a DC offset $-E_{WE} - V_{bias}$, which is removed during the software lock-in detection of the amplitude of i_{sig}.

The circuit was implemented on a PCB with the same chips as those used in the LAPS-grounded control circuit in Figure 3a. For unification of LAPS-grounded and WE-grounded control circuits, see Appendix A.

4. Measurement Setup

The functionalities of the developed circuits were tested in a measurement cell shown schematically in Figure 4. The measurement cell is made of plexiglass, which accommodates 3 mL of test solution, an Ag/AgCl RE (RE-1B, BAS Inc., Tokyo, Japan), and two Pt wires as the WE and the CE. The bottom of the measurement cell has an opening with a diameter of 10 mm, to be sealed with the LAPS surface with an O-ring. The distance between the WE and the LAPS surface is 5 mm. The LAPS sensor plate has the same layer structure as those used in our previous studies [17]; it is made of n-type Si with a resistivity of 1–10 Ωcm, with a size of 17.5 mm × 17.5 mm and a thickness of 200 μm. A 50 nm thick thermal oxide and a 50 nm thick Si_3N_4 are deposited in this order on the front surface, and a gold electrode is evaporated on the rear surface. As a light source for exciting photocarriers, a visible light-emitting diode (LED) is advantageous for the ease of operation and the availability of ultrahigh brightness. In our setup, a red LED with a peak wavelength of 630 nm (L5-EKR2530-12500, Full Sun Optotech, Taichung City, Taiwan) shines on the rear surface of the LAPS to generate a photocurrent signal. The LED current is sinusoidally modulated at 2500 Hz with peak currents being 0 and 20 mA. The modulation signal is supplied by a digital function generator (DF1906, NF Corporation, Yokohama, Japan), which has a frequency accuracy of 25 ppm. The input/output parameters of the control circuit are supplied/read out by a 16-bit digital-to-analog/analog-to-digital converter (DAC/ADC, USB-6002, National Instruments/Emerson Electric, Austin, TX, USA), which has a timebase accuracy of 100 ppm. The LAPS signal is digitized at a sampling rate of 50 kHz, and the amplitude of its frequency component at 2500 Hz is numerically calculated from a sequence of 10,000 sampling points obtained in 200 ms. Considering the high accuracies of both the modulation frequency and the sampling frequency, the software lock-in detection internally generates sine and cosine functions of the reference frequency based on the sampling period instead of a reference signal from the digital function generator. The experiments were conducted using homemade software written with LabVIEW® 2024 (National Instruments/Emerson Electric, Austin, TX, USA).

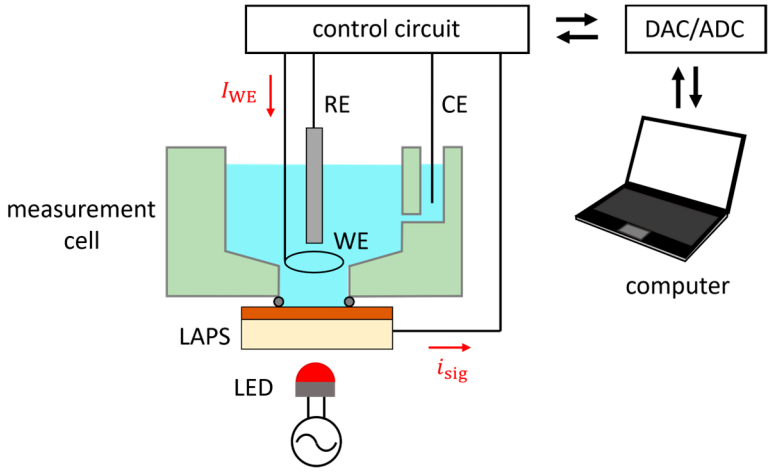

Figure 4. Schematic of the measurement cell for demonstration of potentiostatic/galvanostatic polarization and simultaneous LAPS measurement. The measurement cell is made of plexiglass, which accommodates 3 mL of test solution in contact with the LAPS surface. The four electrodes (LAPS, RE, WE, and CE) are connected to the control circuit developed in this study. DAC, digital-to-analog converter; ADC, analog-to-digital converter.

5. Results and Discussion

5.1. Current-Voltage Curves of LAPS

The current-voltage curves of the LAPS sensor plate were obtained using the LAPS-grounded control circuit operated in the PS mode. The bias voltage V_{bias} applied to the RE with respect to the LAPS was varied in the range of −2 to 0 V with a step of 5 mV, which corresponded to the transition of the state of the insulator–semiconductor interface from inversion to depletion to accumulation. After each stepwise change of V_{bias}, sampling of i_{sig} was started after a delay of 50 ms to ensure completion of charging/discharging the capacitance of the LAPS sensor plate under the updated bias. The value of E_{WE} vs. RE was fixed at 0 V so that there was no faradaic current throughout this measurement. Figure 5a shows the i_{sig}–V_{bias} curves for a series of pH buffer solutions (Titrisol®, Merck, Darmstadt, Germany) with pH 4 to 10. A horizontal shift of the curves along the voltage axis was observed, indicating the pH dependence of the potential difference between the sensing surface and the solution. For each curve, the bias voltage $V_{1/2}$, at which the current became half the maximum, was calculated and plotted versus pH, as shown in Figure 5b, which gave the slope sensitivity of this LAPS sensor plate 52.1 mV/pH.

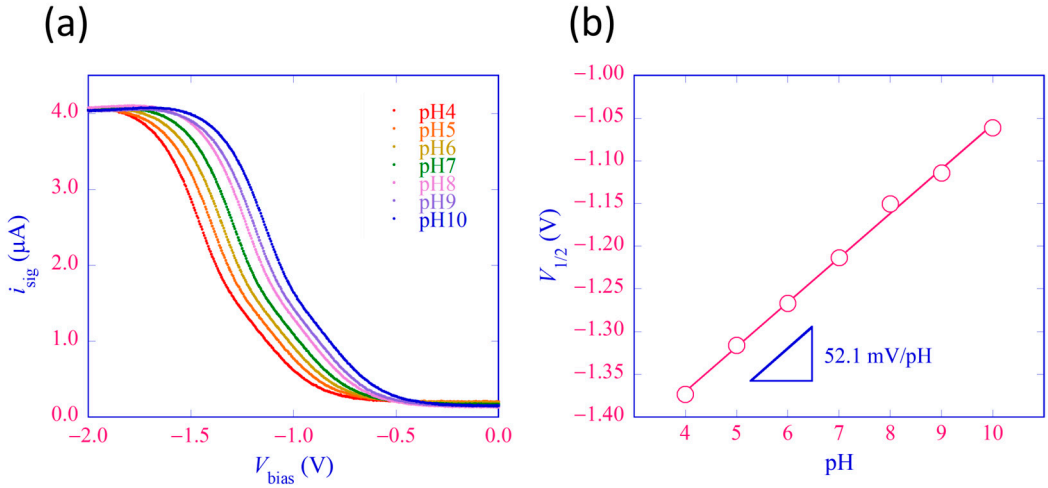

Figure 5. Characterization of the LAPS sensor plate using the LAPS-grounded control circuit in Figure 3a operated in the PS mode. The value of E_{WE} was set to 0 V vs. RE during the measurement. (**a**) The current-voltage (i_{sig}–V_{bias}) characteristics measured for a series of pH buffer solutions with different pH values from 4 to 10. (**b**) A calibration plot of the LAPS sensor plate. The value of the bias voltage $V_{1/2}$, at which the LAPS signal i_{sig} equal to half the maximum, is plotted as a function of pH.

5.2. Polarization and LAPS Measurement with LAPS-Grounded Control Circuit

An example of a polarization curve was obtained using the LAPS-grounded control circuit operated in the PS mode. The test solution was 3 mL of 0.1 M Na_2SO_4. The value of E_{WE} was varied between −1 V and +1.5 V at a rate of ±12.5 mV/s in both directions, and I_{WE} was recorded. Figure 6a shows the obtained I_{WE}–E_{WE} curves, in which electrolysis of water is observed at higher and lower potentials.

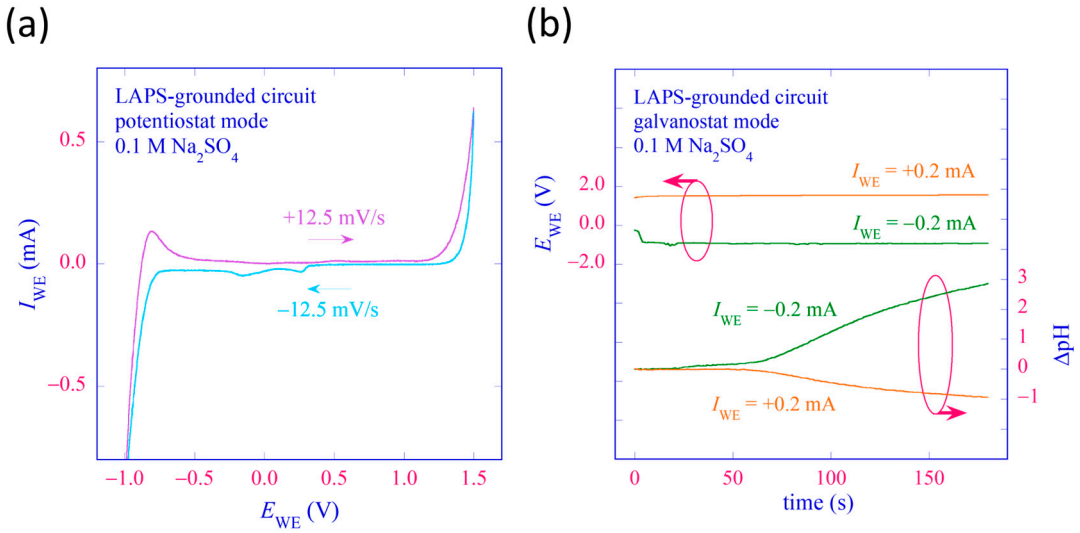

Figure 6. Results of polarization experiments conducted and recorded with a LAPS-grounded control circuit. The test solution was 0.1 M Na_2SO_4, and the WE was a Pt wire placed at a distance of 5 mm from the LAPS surface, as shown in Figure 4. (**a**) A polarization curve recorded in the PS mode. (**b**) Simultaneous recording of E_{WE} and ΔpH in the course of galvanostatic polarization with I_{WE} = ±0.2 mA.

The LAPS-grounded control circuit was then operated in the GS mode, and the WE was galvanostatically polarized both anodically and cathodically using the same test solution. The value of I_{WE} was controlled at ±0.2 mA, and the value of E_{WE} during galvanostatic polarization was recorded. At the same time, i_{sig} was recorded under a fixed value of V_{bias}

= −1.3 V, which was in the middle of the transition region of the i_{sig}–V_{bias} curve of the test solution. The variation of i_{sig} was converted into the potential shift using the slope of the i_{sig}–V_{bias} curve, −7.03 μA/V at V_{bias} = −1.3 V, and the potential shift was further converted into the pH change using the slope sensitivity of the LAPS sensor plate, 52.1 mV/pH. For a detailed discussion of this conversion, see Appendix B. Figure 6b shows the result of this experiment. When the WE was an anode, the pH value decreased due to the anodic reaction: $2H_2O \rightarrow O_2 + 4H^+ + 4e^-$ after an initial delay of ca. 60 s. The initial delay was the time needed for protons generated at the WE to reach the LAPS surface by diffusion, which was verified by coloring the solution with methyl orange. Contrarily, when the WE was a cathode, the pH value increased due to the cathodic reaction: $2H_2O + 2e^- \rightarrow H_2 + 2OH^-$. These results demonstrated the functionalities of the LAPS-grounded control circuit, which can polarize the WE both potentiostatically and galvanostatically, and record the resulting pH change on the LAPS surface at the same time.

5.3. Polarization and LAPS Measurement with WE-Grounded Control Circuit

Similar experiments were also carried out with a WE-grounded control circuit to test its functionality. This time, the test solution was 3 mL of 0.01 M KNO_3. Figure 7a shows an example of a polarization curve obtained by varying E_{WE} in the PS mode at a rate of ±100 mV/s in the range between −0.5 V and +1.5 V. Electrolysis of water is observed at higher potentials. Figure 7b shows the temporal changes of E_{WE} and ΔpH during anodic polarization of the WE in the GS mode with I_{WE} = +0.1 mA and +1.0 mA. The value of V_{bias} for LAPS measurement was fixed at −1.4 V. Lowering of pH due to the anodic reaction at different rates dependent on I_{WE} was observed, demonstrating the functionality of the WE-grounded control circuit.

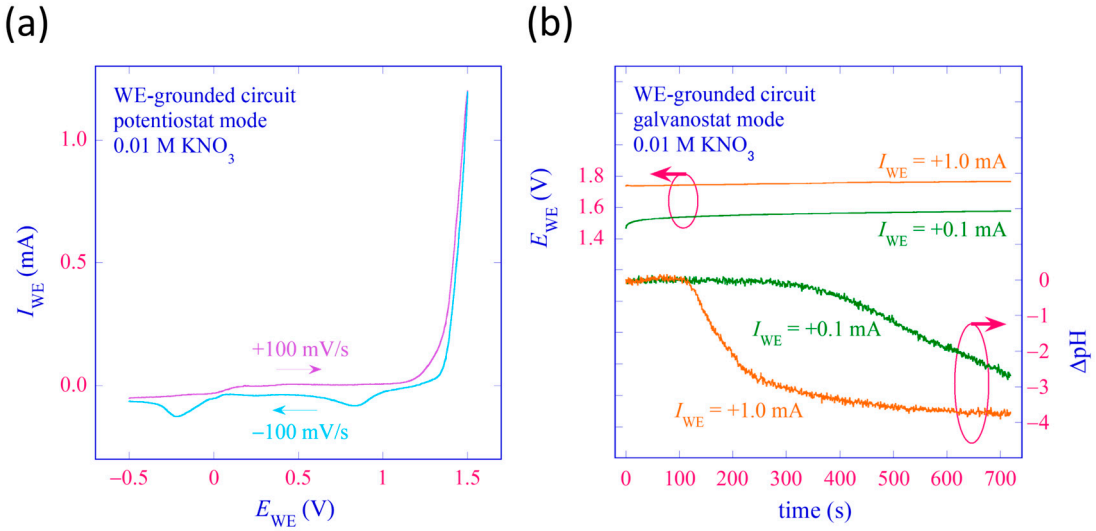

Figure 7. Results of polarization experiments conducted and recorded with a WE-grounded control circuit. The test solution was 0.01 M KNO_3, and the WE was a Pt wire placed at a distance of 5 mm from the LAPS surface, as shown in Figure 4. (**a**) A polarization curve recorded in the PS mode. (**b**) Simultaneous recording of E_{WE} and ΔpH in the course of galvanostatic polarization with I_{WE} = +0.1 mA and +1.0 mA.

5.4. Interference between Polarization and LAPS Measurement

In this section, the possibility of interference between polarization and LAPS measurement is discussed. In the four-electrode system, both I_{WE} and i_{sig} are ideally collected entirely by the CE, which has a low input impedance. When the WE and the LAPS are placed in close proximity, however, there may be crosstalk between them.

As the LAPS surface is insulated, the DC component of the current flowing out of the WE, I_{WE} will not enter the LAPS and will be collected only by the CE. When I_{WE} contains

an AC component, either due to fluctuation of the electrochemical reaction on the WE surface or due to electrical noise, it may enter the LAPS via capacitive coupling between the solution and the semiconductor layer of the LAPS. Its influence on the measurement of i_{sig} can, however, be mostly eliminated during the software lock-in detection of i_{sig} at the frequency of modulation. Therefore, the influence of polarization on the LAPS measurement can be ignored in most cases.

Conversely, the alternating current flowing out of the LAPS surface, $-i_{sig}$ in our notation, can enter the WE when it is placed in close proximity to the LAPS surface. In the GS mode, the control circuit has a high impedance at the output terminal connected to the WE and, therefore, can reject this crosstalk. In the PS mode, however, the control circuit has a low impedance at the output terminal, and the current enters the circuit. Whether this crosstalk can be a problem or not depends on the relative magnitudes of I_{WE} and i_{sig}. Additionally, a coil may be inserted in series with the WE to reject an alternating current.

Yet another form of interference may occur when V_{bias} is changed during measurement. The bias voltage applied between the RE and the LAPS, V_{bias}, is either kept constant or varied depending on the purpose of LAPS measurement. When the temporal resolution has priority, V_{bias} is fixed, and the temporal change of i_{sig} is recorded and converted into ΔpH as was done in Figures 6b and 7b. When the precision in determining the activity of the analyte is prioritized, V_{bias} is varied in a certain range to obtain the i_{sig}–V_{bias} curve such as the one in Figure 5a, from which the voltage shift can be more precisely calculated. In the latter case, V_{bias} is changed stepwise during LAPS measurement. In the case of measurement in Figure 5a, for example, the step was 5 mV. When V_{bias} is abruptly changed, there will be a transient current charging/discharging the capacitance of the LAPS. In addition, it will disturb the feedback loop controlling E_{WE} in the PS mode or I_{WE} in the GS mode until the fluctuation is settled down.

The influence of the change of V_{bias} on the potentiostatic/galvanostatic polarization was experimentally assessed using the developed circuits. The test solution was 3 mL of 0.1 M KNO_3, and the target values of E_{WE} in the PS mode and I_{WE} in the GS mode were set at 0. Then, V_{bias} was abruptly changed from −1000 mV to −980 mV by a step of 20 mV, and the resulting fluctuations of E_{WE} and I_{WE} were recorded at a sampling rate of 5 MS/s using a digital storage oscilloscope (MSO22, Tektronics, Beaverton, OR, USA) as shown in Figure 8. The disturbance continued for ca. 10 μs until the control recovered. The fluctuations of E_{WE} in the PS mode and I_{WE} in the GS mode were ca. 10 mV and 20 μA, respectively. These values are small enough for corrosion experiments [15–17], but if a higher precision is required, V_{bias} must be changed by a smaller step. It should be noted that the duration and the magnitude of disturbance would depend on the details of the electrochemical system as well as the implementation of the control circuit.

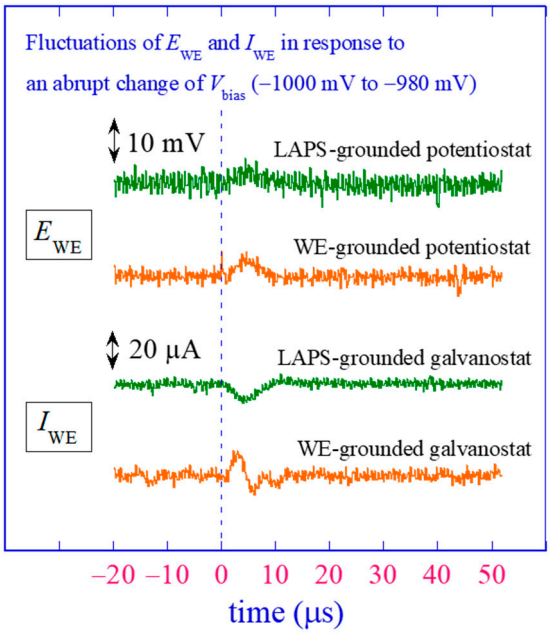

Figure 8. Assessment of the influence of LAPS measurement on polarization. The target values of E_{WE} (in the PS mode) and I_{WE} (in the GS mode) were set at 0, and the value of V_{bias} applied between the RE and the LAPS was abruptly changed from −1000 mV to −980 mV. Fluctuations of E_{WE} and I_{WE} in response to this stepwise change of V_{bias} were recorded at a sampling rate of 5 MS/s.

6. Conclusions

In this study, a four-electrode system was proposed, in which a LAPS was included as the fourth electrode for potentiometric sensing of the target analyte in the course of an electrochemical reaction taking place on the surface of the WE. Control circuits with different grounding modes that can simultaneously conduct potentiostatic/galvanostatic polarization and LAPS measurement were designed and developed, and their functionalities were verified in a demonstration of the temporal recording of pH change due to anodic/cathodic reactions in electrolysis of water. The possibility of interference between polarization and LAPS measurement was discussed in detail.

The integration of a LAPS into a conventional three-electrode system will allow simultaneous recording of the electrochemical reaction on the WE surface and the spatiotemporal distribution of the target analyte in the vicinity of the WE surface. This measurement system is expected to be useful for the analysis of dynamics involving not only electrochemistry but also reaction and diffusion in the solution.

Finally, one of the interesting applications of the proposed four-electrode system would be the combination of amperometric and potentiometric sensors [35–40], using an amperometric sensor as the WE and a LAPS as the fourth electrode. For example, the enzymatic oxidation of glucose catalyzed by glucose oxidase produces gluconic acid and hydrogen peroxide. While the latter is amperometrically detected, the pH change due to the former can be recorded to correct for the influence of pH. For such applications, where I_{WE} can be even smaller than i_{sig}, the design and implementation of the control circuit would require further sophistication and optimization.

Author Contributions: Conceptualization, T.Y.; methodology, T.Y., R.I., and K.-i.M.; software, T.Y., R.I., and K.-i.M.; investigation, T.Y. and R.I.; writing—original draft preparation, T.Y.; writing—review and editing, T.Y. and K.-i.M. All authors have read and agreed to the published version of the manuscript.

Funding: This research was funded by JSPS KAKENHI Grant Number JP23K23368.

Institutional Review Board Statement: Not applicable.

Data Availability Statement: Data are contained within the article.

Conflicts of Interest: The authors declare no conflicts of interest.

Appendix A

Taking advantage of the similarities between the LAPS-grounded and WE-grounded control circuits in Figure 3, they can be unified, as shown in Figure A1.

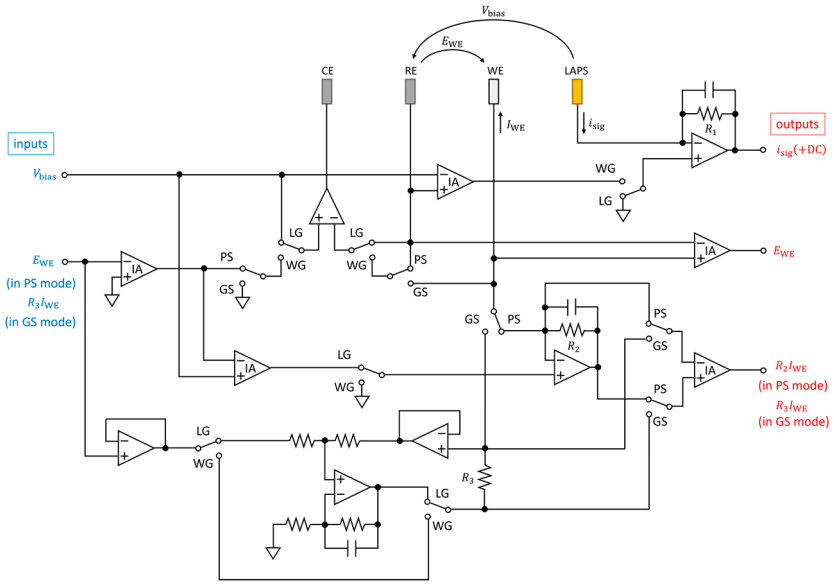

Figure A1. A unified control circuit that can be switched between the LAPS-grounded mode and the WE-grounded mode. In each grounding mode, the operation mode can be switched between the PS mode and the GS mode. LG, LAPS-grounded; WG, WE-grounded; PS, potentiostat; GS, galvanostat; IA, instrumentation amplifier.

Appendix B

In the polarization experiments shown in Figures 6b and 7b, the photocurrent signal i_{sig} was recorded under a constant value of V_{bias}, and the temporal variation of i_{sig} was converted into ΔpH using the slope of the transition region of the i_{sig}–V_{bias} curve such as the one shown in Figure 5a. Here, the linearity of the transition region was implicitly assumed, which, in fact, is not accurate when the variation of i_{sig} is not small. Particularly, as can be seen in Figure 5a, the slope becomes considerably smaller as the current decreases. The actual lowering of pH is, therefore, larger than those shown in Figures 6b and 7b, which also explains the asymmetry of ΔpH curves for anodic and cathodic polarization in Figure 6b. For a more accurate conversion of i_{sig} into ΔpH, the shape of the i_{sig}–V_{bias} curve must be taken into account.

References

1. Hafeman, D.G.; Parce, J.W.; McConnell, H.M. Light-addressable potentiometric sensor for biochemical systems. *Science* **1988**, *240*, 1182–1185. [CrossRef] [PubMed]
2. Owicki, J.C.; Bousse, L.J.; Hafeman, D.G.; Kirk, G.L.; Olson, J.D.; Garrett Wada, H.; Wallace Parce, J. The light-addressable potentiometric sensor: Principles and biological applications. *Annu. Rev. Biophys. Biomol. Struct.* **1994**, *23*, 87–113. [CrossRef] [PubMed]
3. Yoshinobu, T.; Miyamoto, K.; Werner, C.F.; Poghossian, A.; Wagner, T.; Schöning, M.J. Light-addressable potentiometric sensors for quantitative spatial imaging of chemical species. *Annu. Rev. Anal. Chem.* **2017**, *10*, 225–246. [CrossRef] [PubMed]
4. Yoshinobu, T.; Schöning, M.J. Light-addressable potentiometric sensors for cell monitoring and biosensing. *Curr. Opin. Electrochem.* **2021**, *28*, 100727. [CrossRef]
5. Liu, Y.; Zhu, P.; Liu, S.; Chen, Y.; Liang, D.; Wang, M.; Du, L.; Wu, C. The Light-addressable potentiometric sensor and its application in biomedicine towards chemical and biological sensing. *Chemosensors* **2022**, *10*, 156. [CrossRef]

6. Meng, Y.; Chen, F.; Wu, C.; Krause, S.; Wang, J.; Zhang, D.-W. Light-addressable electrochemical sensors toward spatially resolved biosensing and imaging applications. *ACS Sens.* **2022**, *7*, 1791–1807. [CrossRef]
7. Luo, J.; Liu, S.; Chen, Y.; Tan, J.; Zhao, W.; Zhang, Y.; Li, G.; Du, Y.; Zheng, Y.; Li, X.; et al. Light addressable potentiometric sensors for biochemical imaging on microscale: A review on optimization of imaging speed and spatial resolution. *ACS Omega* **2023**, *8*, 42028–42044. [CrossRef]
8. Nakao, M.; Yoshinobu, T.; Iwasaki, H. Scanning-laser-beam semiconductor pH-imaging sensor. *Sens. Actuators B* **1994**, *20*, 119–123. [CrossRef]
9. Uchida, H.; Zhang, W.Y.; Katsube, T. High-speed chemical image sensor with digital LAPS system. *Sens. Actuators B* **1996**, *34*, 446–449. [CrossRef]
10. Miyamoto, K.; Kuwabara, Y.; Kanoh, S.; Yoshinobu, T.; Wagner, T.; Schöning, M.J. Chemical image scanner based on FDM-LAPS. *Sens. Actuators B* **2009**, *137*, 533–538. [CrossRef]
11. Chen, L.; Zhou, Y.; Jiang, S.; Kunze, J.; Schmuki, P.; Krause, S. High resolution LAPS and SPIM. *Electrochem. Commun.* **2010**, *12*, 758–760. [CrossRef]
12. Wagner, T.; Werner, C.F.; Miyamoto, K.; Schöning, M.J.; Yoshinobu, T. Development and characterisation of a compact light-addressable potentiometric sensor (LAPS) based on the digital light processing (DLP) technology for flexible chemical imaging. *Sens. Actuators B* **2012**, *170*, 34–39. [CrossRef]
13. Das, A.; Lin, Y.H.; Lai, C.S. Miniaturized amorphous-silicon based chemical imaging sensor system using a mini-projector as a simplified light-addressable scanning source. *Sens. Actuators B* **2014**, *190*, 664–672. [CrossRef]
14. Das, A.; Chen, T.C.; Yang, C.M.; Lai, C.S. A high-speed, flexible-scanning chemical imaging system using a light-addressable potentiometric sensor integrated with an analog micromirror. *Sens. Actuators B* **2014**, *198*, 225–232. [CrossRef]
15. Miyamoto, K.; Sakakita, S.; Wagner, T.; Schöning, M.J.; Yoshinobu, T. Application of chemical imaging sensor to in-situ pH imaging in the vicinity of a corroding metal surface. *Electrochim. Acta* **2015**, *183*, 137–142. [CrossRef]
16. Miyamoto, K.; Sakakita, S.; Werner, C.F.; Yoshinobu, T. A modified chemical imaging sensor system for real-time pH imaging of accelerated crevice corrosion of stainless steel. *Phys. Satus Solidi A* **2018**, *215*, 1700963. [CrossRef]
17. Miyamoto, K.; Hiramitsu, R.; Werner, C.F.; Yoshinobu, T. Simultaneous in situ imaging of pH and surface roughening during the progress of crevice corrosion of stainless steel. *Sensors* **2022**, *22*, 2246. [CrossRef]
18. Bucher, V.; Brunner, B.; Leibrock, C.; Schubert, M.; Nisch, W. Electrical properties of a light-addressable microelectrode chip with high electrode density for extracellular stimulation and recording of excitable cells. *Biosens. Bioelectron.* **2001**, *16*, 205–210. [CrossRef]
19. Colicos, M.A.; Collins, B.E.; Sailor, M.J.; Goda, Y. Remodeling of synaptic actin induced by photoconductive stimulation. *Cell* **2001**, *107*, 605–616. [CrossRef]
20. Starovoytov, A.; Choi, J.; Seung, H.S. Light-directed electrical stimulation of neurons cultured on silicon wafers. *J. Neurophysiol.* **2005**, *93*, 1090–1098. [CrossRef]
21. Suzurikawa, J.; Takahashi, H.; Kanzaki, R.; Nakao, M.; Takayama, Y.; Jimbo, Y. Light-addressable electrode with hydrogenated amorphous silicon and low-conductive passivation layer for stimulation of cultured neurons. *Appl. Phys. Lett.* **2007**, *90*, 093901. [CrossRef]
22. Hagiwara, T.; Takazawa, M.; Uchida, H.; Hasegawa, Y.; Yaji, T. An amperometric sensor for chemical imaging using photoconductive organic film. *IEICE Trans. Electron.* **2008**, *91*, 1863–1868. [CrossRef]
23. Arai, H.; Goto, D.; Hasegawa, Y.; Uchida, H. Study on the two-dimensional chemical sensor using a photoconductive polymer film. *IEEJ Trans. Sens. Micromach.* **2013**, *133*, 290–296. [CrossRef]
24. Shichijo, M.; Hasegawa, Y.; Uchida, H. Study of detection method for collagenase enzyme reaction using two dimensional electrochemical sensor. *Electron. Commun. Jpn.* **2020**, *103*, 90–96. [CrossRef]
25. Kosugi, K.; Uchida, H. Study of LAAS sensitivity using back surface electric field. *IEEJ Trans. Sens. Micromach.* **2021**, *141*, 14–20. [CrossRef]
26. Kosugi, K.; Hasegawa, Y.; Uchida, H. Light-addressable amperometric sensor with counter and working electrodes of the same material. *IEEJ Trans. Electr. Electron. Eng.* **2021**, *16*, 478–485. [CrossRef]
27. Miyairi, A.; Hasegawa, Y.; Uchida, H. Measurement of acetylcholinesterase using a two-dimensional electrochemical sensor LAAS. *Electron. Commun. Jpn.* **2023**, *106*, e12425. [CrossRef]
28. Choudhury, M.H.; Ciampi, S.; Yang, Y.; Tavallaie, R.; Zhu, Y.; Zarei, L.; Gonçalesa, V.R.; Gooding, J.J. Connecting electrodes with light: One wire, many electrodes. *Chem. Sci.* **2015**, *6*, 6769–6776. [CrossRef]
29. Yang, Y.; Ciampi, S.; Zhu, Y.; Gooding, J.J. Light-activated electrochemistry for the two-dimensional interrogation of electroactive regions on a monolithic surface with dramatically improved spatial resolution. *J. Phys. Chem. C* **2016**, *120*, 13032–13038. [CrossRef]
30. Kashi, M.B.; Silva, S.M.; Yang, Y.; Gonçales, V.R.; Parker, S.G.; Barfidokht, A.; Ciampi, S.; Gooding, J.J. Light-activated electrochemistry without surface-bound redox species. *Electrochim. Acta* **2017**, *251*, 250–255. [CrossRef]
31. Vogel, Y.B.; Gonçales, V.R.; Gooding, J.J.; Ciampi, S. Electrochemical microscopy based on spatial light modulators: A projection system to spatially address electrochemical reactions at semiconductors. *J. Electrochem. Soc.* **2018**, *165*, H3085–H3092. [CrossRef]
32. Wu, F.; Zhou, B.; Wang, J.; Zhong, M.; Das, A.; Watkinson, M.; Hing, K.; Zhang, D.W.; Krause, S. Photoelectrochemical imaging system for the mapping of cell surface charges. *Anal. Chem.* **2019**, *91*, 5896–5903. [CrossRef] [PubMed]

33. Zhou, B.; Das, A.; Zhong, M.; Guo, Q.; Zhang, D.W.; Hing, K.A.; Sobrido, A.J.; Titirici, M.M.; Krause, S. Photoelectrochemical imaging system with high spatiotemporal resolution for visualizing dynamic cellular responses. *Biosens. Bioelectron.* **2021**, *180*, 113121. [CrossRef] [PubMed]
34. Zhou, B.; Jiang, Y.; Guo, Q.; Das, A.; Sobrido, A.B.J.; Hing, K.A.; Zayats, A.V.; Krause, S. Photoelectrochemical detection of calcium ions based on hematite nanorod sensors. *ACS Appl. Nano Mater.* **2022**, *5*, 17087–17094. [CrossRef] [PubMed]
35. Kimura, J.; Murakami, T.; Kuriyama, T.; Karube, I. An integrated multibiosensor for simultaneous amperometric and potentiometric measurement. *Sens. Actuators* **1988**, *15*, 435–443. [CrossRef]
36. Schelter, W.; Gumbrecht, W.; Montag, B.; Sykora, U.; Erhardt, W. Combination of amperometric and potentiometric sensor principles for on-line blood monitoring. *Sens. Actuators B* **1992**, *6*, 91–95. [CrossRef]
37. Chen, Z.-L.; Hibbert, D.B. Simultaneous amperometric and potentiometric detection of sugars, polyols and carboxylic acids in flow systems using copper wire electrodes. *J. Chromatogr. A* **1997**, *766*, 27–33. [CrossRef]
38. Schöning, M.J.; Krause, R.; Block, K.; Musahmeh, M.; Mulchandani, A.; Wang, J. A dual amperometric/potentiometric FIA-based biosensor for the distinctive detection of organophosphorus pesticides. *Sens. Actuators B* **2003**, *95*, 291–296. [CrossRef]
39. Izquierdo, J.; Nagy, L.; Santana, J.J.; Nagy, G.; Souto, R.M. A novel microelectrochemical strategy for the study of corrosion inhibitors employing the scanning vibrating electrode technique and dual potentiometric/amperometric operation in scanning electrochemical microscopy: Application to the study of the cathodic inhibition by benzotriazole of the galvanic corrosion of copper coupled to iron. *Electrochim. Acta* **2011**, *58*, 707–716. [CrossRef]
40. Filotás, D.; Fernández-Pérez, B.M.; Izquierdo, J.; Nagy, L.; Nagy, G.; Souto, R.M. Combined amperometric/potentiometric probes for improved chemical imaging of corroding surfaces using Scanning Electrochemical Microscopy. *Electrochim. Acta* **2016**, *221*, 48–55. [CrossRef]